Proceedings of ICAPP 2015
May 03-06, 2015 - Nice (France)
Paper 15239

Modelling of Flow and Heat Transfer in Spent Fuel Cooling Ponds

Reaz Hasan*, Jenna Tudor and Ahmed Ramadan
Department of Mechanical and Construction Engineering
Northumbria University Newcastle
Newcastle Upon Tyne NE1 8ST, UK
**Tel: 0191 243 7233, Email:reaz.hasan@northumbria.ac.uk*

Abstract – *With increased interest in Nuclear power generation and the issues of storing legacy fuels being apparent there is a real need to understand the heat transfer mechanisms involved in storing spent fuel within water filled cooling ponds. This paper draws together the findings from several projects exploring the fundamental transport mechanisms in similar systems and, in particular, highlights the challenges encountered during numerical simulation. The projects from which conclusions were drawn are (a) Computational Fluid Dynamic (CFD) investigation of overall pond flow and heat transfer; (b) Modelling of evaporation from the pond and its interaction with external atmospheric conditions and (c) Investigation of possible overheating based on elementary thermodynamics.*

I. INTRODUCTION

At the start of 2006, nuclear reactors around the world discharged a huge amount of Spent Nuclear Fuel (SNF) which approximately amounted 290,000 tHM (metric tons of heavy metal), with about 30% of this quantity going for reprocessing. The expected amount of SNF to be produced by 2020 will almost double with just quarter of the total amount that can be reprocessed[1]. With respect to these circumstances, developing such ponds became essential issues in the nuclear fuel cycle.

There are two main issues to be considered in the developing process of such systems. First is the safety aspect as a result of residual radio-activity and risk of overheating which represent serious harm to the public and the environment as what happened in recent Fukushima incident[2]. Second is the continuous need of management action during the long-term storage of SNF. Clearly, a more efficient and optimised fuel stacking would improve the current scenario[3].

Kim et al.[3] have reported an investigation on the heat transfer and flow characteristics in storage vaults as used in South Korea. The focus of their work was on improving space efficiency to meet the ever growing numbers of SNF. Yanagi et al.[4] have considered heat loss and water temperature variation in a small fuel pit of size 10m x 15m x 12m. The CFD results were validated against a small version of comparable flow situation and suggested useful

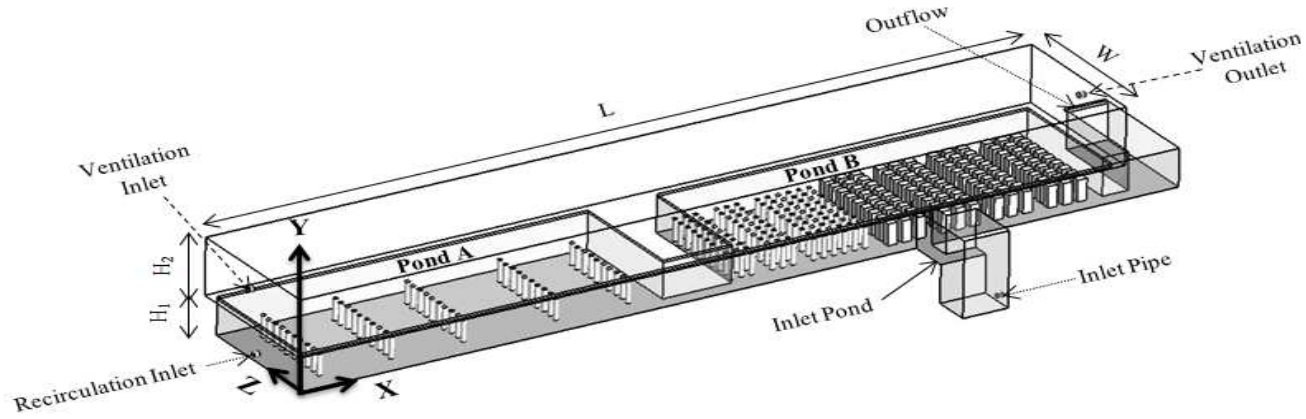

Fig. 1. The computational domains showing three ponds, fuels and humid air section.

models to handle the evaporation flux from the top surface of the water pond. In an adjoining paper, the same authors[5] have analysed the water temperature rise in a shutdown of its cooling systems. Again, the simulations were based on a small cooling pond and hence the financial efficiency of such systems may not be applicable for larger size ponds whose lengths could be several times more. To the best of our knowledge, full scale numerical simulations of such systems have possibly not been published due to the information being commercially sensitive. The flow and heat transfer characteristics can be quite complex due to large variation of velocity scales in the pond. Fig. 1 shows a computational model of the SNF cooling pond house considered in this study. It can be seen that the lower part represents the actual pond of dimension L=170 m, W=28 m and H_1 = 8 m. The ponds are filled with racks which contain various types of fuel cans. The upper half of height H_2 = 9 m represents the housing filled with humid air. The flow parameters are largely influenced by the design as well as by the stacking arrangement and age of the fuels. As with any other thermo-fluidic process, investigation in SNF ponds can be carried out by experimental, numerical or (in some cases) by analytical/empirical equations. From the limited published work, it is obvious that conducting experiments in SNF ponds is extremely difficult due to its huge size as well as due to the hazard associated with radiation contamination. On the other hand, numerical methods such as CFD can be used, in principle, to address the fluid flow and heat transfer scenario using computers. The CFD methodology is now well established, but the available literature indicates that the investigations on SNF ponds is still very limited[3]. The third approach is rather simplistic where bulk approaches are taken to calculate worst case scenarios of 'pond drying'. Such calculations are usually based on oversimplified assumptions and the accuracy of the results is questionable and may even lead to undue negative publicity.

Based on the above discussion we can emphasise that CFD is perhaps a very appropriate approach in optimising the design of cooling ponds. The aim this paper is to critique our own modelling strategies for various aspects in relation to the flow, heat and mass transfer in the context of cooling pond for spent fuel. This paper raises several practical issues in relation to the CFD investigation of such system and suggests pragmatic route map in order that a workable and reliable numerical model can be achieved. The conclusions and recommendations presented in this paper are mainly based on our own on-going research experiences carried out for the last two years.

.

II. NUMERICAL SIMULATION OF THE FULL POND

For this investigation, the lower part of the pond house has been considered. As shown in Fig. 1, the computational domain (up to height H_1) is made up of three ponds identified as Pond A, Pond B and the Inlet Pond. The main flow exits through Pond B and there is also arrangement for a recirculating flow through Pond A, more details can be found in Robinson et al.[6]. We will concentrate on interesting flow features highlighting the complexity as well as focusing on the flexibility of CFD method for operational optimisation.

II.A. Methodology

Steady state simulations were conducted using the commercial CFD package of ANSYS FLUENT[7] where the continuity, momentum and energy equations were solved. It was obvious that most of the domain was dominated by small velocities but there were regions where Rayleigh number could be high and, hence, the k-ε turbulence model was incorporated. Buoyancy forces were also considered in the calculation by selecting the appropriate material properties and including the gravity force in the momentum equation. This simulation consists of two scenarios: with and without recirculation of the exit flow. In the first case, velocity boundary condition was employed at the inlet pipe with uniform velocity corresponding to flow rate of 4 kg/sec. For the second case, an additional inlet was defined at the re-circulation inlet. At the racks surfaces, convective boundary conditions were applied with heat transfer coefficient of 16 W/m^2K and heat flux of 1.04 kW/m^3. The top surface was considered as symmetry which allowed a heat loss of 20%. All other surfaces were assumed to be no-slip walls.

II.B. Results and Discussion

Three dimensional streamlines of the pond are shown in Fig 2. At the bottom of the inlet pond, the cooling water begins its journey and then rises up as helical 'twisted plumes' and moves towards the exit plane in pond B due to the favourable pressure gradient. The bulk of the water then makes a further turn spreading along the fuel cans and finally adjusting itself with the outlet section. The buoyancy effect can be seen in some locations within the flow domain mainly in the places far from the primary stream. Fig 3 illustrates the temperature distribution in pond A (before recirculation) through the vertical plane at the mid-section in the transverse Z-direction. The distributions show the temperature gradient in the vertical direction where the highest temperatures are concentrated at the surfaces of racks. These thermal stratifications in the vertical direction act as the drivers to maintain the natural convection current in order to provide a medium for heat transfer.

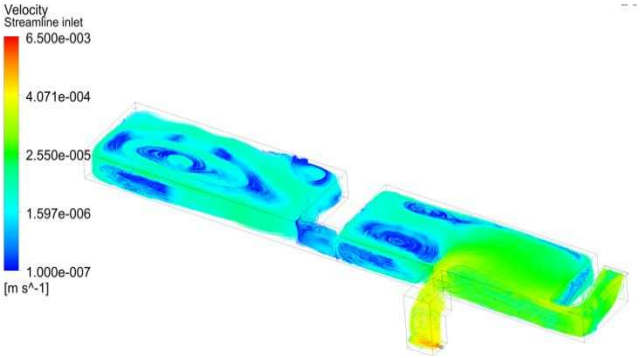

Fig. 2. Three dimensional streamlines for flow field without recirculation.

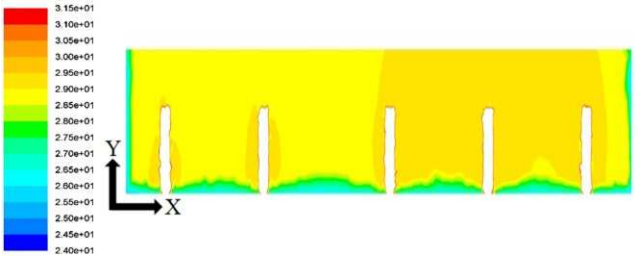

Fig. 3. Thermal stratification in pond A (without re-circulation) along X-direction.

The effect of recirculation was studied in detail[6] and few representative results are presented in this paper. Fig. 4 shows the effect of recirculation on temperature distributions along the X-direction (see Fig. 1). The influence of recirculation is more significant in pond B than pond A at this particular location which is possibly due to the absence of a dominant primary flow stream. However, the overall temperature distribution when recirculation is activated is lower than when it is off.

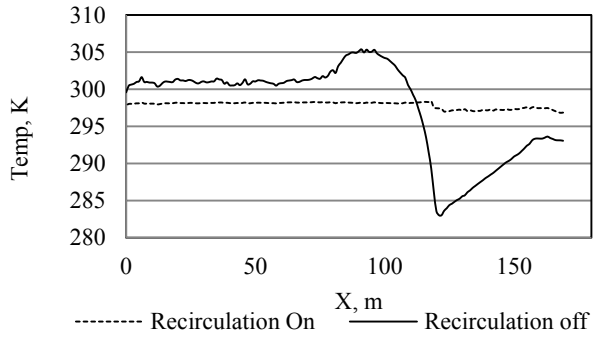

Fig. 4. Temperature variation with and without re-circulation at Y=0.6H_1, Z=0.3W.

After establishing the numerical model, several parametric studies were performed by varying the heat load and the rate of water flow from the inlet without recirculation. In this study, three different configurations were considered where 100% indicates for the original case which was presented earlier. The results of the current study are illustrated in Fig. 5a-b. It can be seen that by reducing the decay heat by 50% and preserving the flow rate, the temperature falls down by almost 7 ^{o}C in pond A, while 50% reduction in the flow rate results in an increase of the temperature by less than 3 ^{o}C. In addition, the temperature distribution in pond A appears to be more uniform than pond B which is probably due to the fact that the fluid motion in Pond A is dominated by natural convection rather than the primary flow in. In contrast, more instability in the temperature gradient can be seen in pond B due to proximity of the primary stream and the outlet.

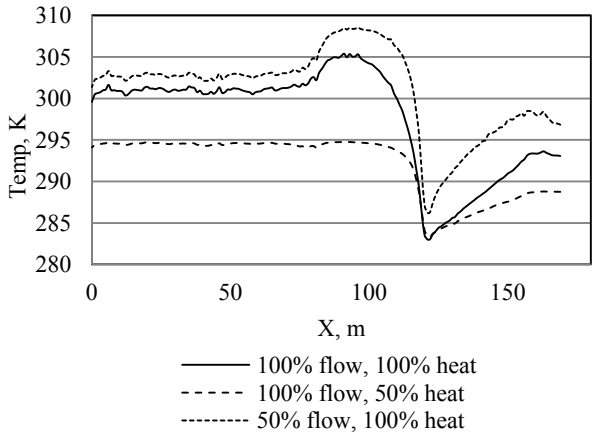

Fig. 5a. Temperature variation with different flow and heat generation rates at Y=0.6H_1, Z=0.1W plane.

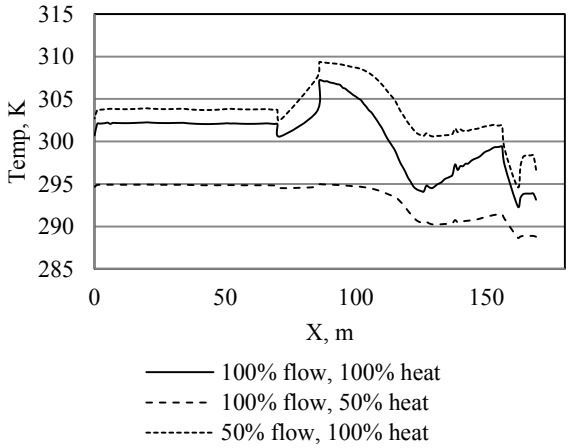

Fig. 5b. Temperature variation with different flow and heat generation rates at Y=0.6H_1 and Z=mid plane. (There is no flow for 70<X<90 and represents void section between ponds)

A more detailed view (micro-scale) of the fluid motion and associated grids can be seen in Figs. 6-7. Clearly, the

typical grids must be fine enough to resolve the near wall fluxes which proved to be very demanding on computing resources. The rising plumes on top of the fuel cans demonstrate the buoyancy effects encountered in the pond.

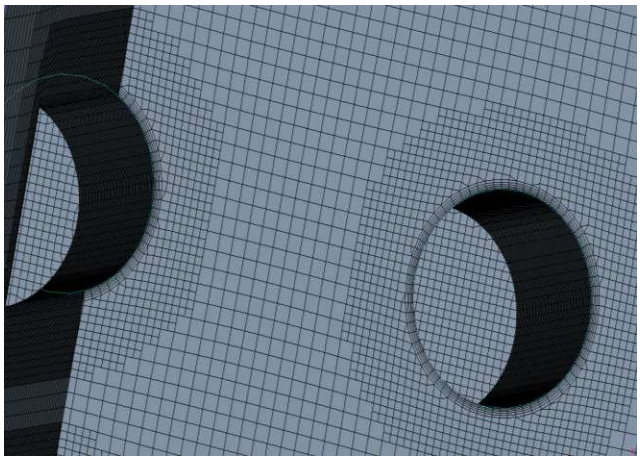

Fig. 6. Typical grids around the fuel containers.

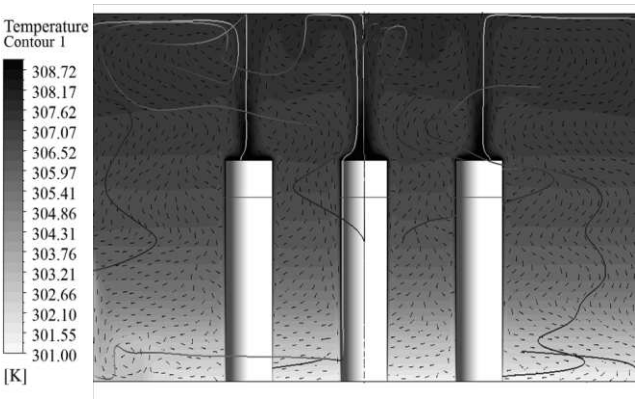

Fig. 7. Typical buoyancy plume.

A detailed analysis as this would prove very demanding on the resources because the number of fuel cans can be several hundred and are of different age (and hence the heat release rates would vary). Also, the spacing between the cans is likely to vary depending on the business. For a full scale model we employed up to about 16M cells and a typical run time was about a week on a dual core PC. It is recognized that the computing time can be very significantly reduced by having a cluster, but from the viewpoint of an industry, this is probably unlikely to happen. One option would be treat the cluster of fuel cans as a porous medium flow. Work is currently underway to scrutinize this approach.

III. NUMERICAL SIMULATION OF HUMID AIR

In this simulation we have considered the volume of humid air above the free water surface and its interaction with the incoming ventilation air. The computational domain represents the upper part of height H_2 as shown in Fig. 1 and a typical mesh is shown in Fig. 8. It can be seen that the meshes are concentrated in a non-uniform fashion in order to capture the steep gradients near the boundaries. The results presented for this investigation were carried out using a $1/10^{th}$ scale model. However, the methodology is not limited by the size effect.

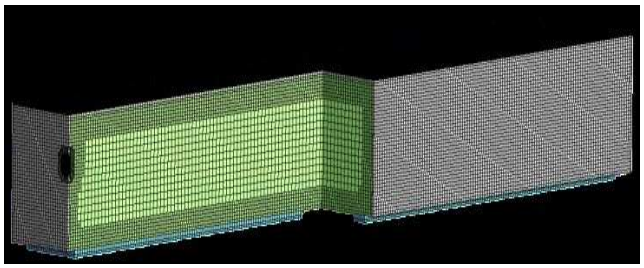

Fig. 8. Section view of grid distribution for computational domain.

III.A. Methodology

The general methodology is similar to what has been presented earlier in section *II.A*. Here, we only highlight the specific features in the context of this simulation. Since the air is humid, species transport (scalar) equation has been incorporated along with energy equation and *k-ε* turbulence model with standard wall functions.

The ventilation inlet was considered to be uniform velocity equivalent to 0.224 Air Change per Hour (ACH) and temperature equal to ambient condition. The ventilation exit boundary condition was chosen to be outflow. At all the walls, except vapour zone walls, convective boundary condition was imposed with heat transfer coefficient of 0.25 W/m^2K and no-slip conditions. For the vapour zone walls, constant temperature was applied which is equal to water temperature. More details can be found in Ramadan et al.[8].

A multi-zone flow model has been used to link between the different zones which is illustrated schematically in Fig. 9. We have considered the domain to be comprised of three zones representing solid zone, humid air zone and vapour zone which represents the very thin layer of air fully saturated in vapour just above the water surface. Including these zones permitted us to apply suitable and realistic boundary conditions and gave us the flexibility to vary the ambient conditions according to seasonal change.

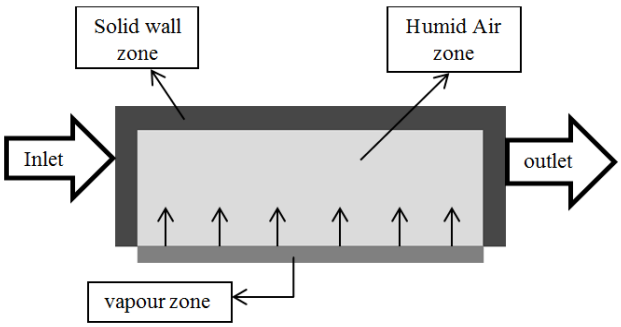

Fig. 9. Schematic of the three domains.

The solid zone was made of concrete with thermal conductivity of 1.4 W/mK. The vapour zone is a very thin layer which represents the boundary layer just above the water surface. Air is considered to be fully saturated with water vapour at the same temperature. This thin boundary layer was introduced to the continuity Eq. (1) as mass source term S_m with $m = m_o - m_i$, where m_i denotes to the absolute humidity at entry (determined from ambient condition) and m_o represents the absolute humidity at exit (assumed fully saturated).

$$\frac{\partial \rho}{\partial t} + \nabla \bullet \left(\rho \vec{v} \right) = S_m \tag{1}$$

In order to preserve the homogeneity of dimensions, S_m is calculated via Eq. (2), where V is the volume of the cell.

$$S_m = \frac{m^{\bullet}}{V} \tag{2}$$

The current methodology was validated against available published data and can be seen in[8]

III.B Results and Discussion

Fig. 10 shows velocity contours on planes of Z= 0.25W and 0.75W, where the velocity magnitudes are very small and velocities with higher values are concentrated near the walls and above the water surface.

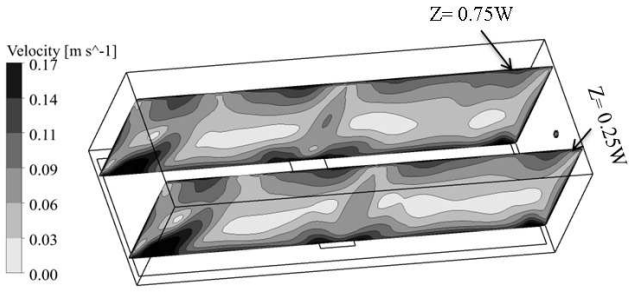

Fig. 10. Velocity contours on Z=0.25W and Z=0.75Wplanes.

Temperature distributions at different planes are shown in Fig. 11. It can be clearly seen that the temperature is lower near the boundaries than above the water surface. This is due to the rising of water vapour which is warmer than the incoming ventilation air.

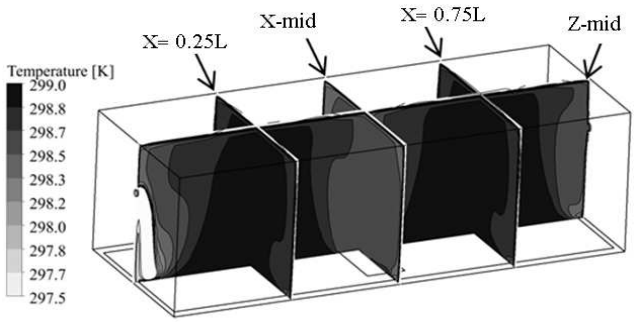

Fig. 11. Temp. contours on Z-mid, X=0.25L, X-mid and X=0.75L planes.

III.C. Parametric Study for Different Climatic Condition

The primary heat losses from the cooling ponds are due to sensible and latent (due to evaporation) heats and were evaluated at different seasonal conditions. In this study we have focused on evaluating the amount of heat loss by means of sensible and latent heat with regard to climate change. Also we have calculated the thermal stratification level within the humid air zone.

Table 1 contains the climate parameters which were considered in the calculations and were incorporated through temperature and relative humidity of ambient air. Fig. 12 represents the amount of both heat loss components from the building body in four different seasons. It can be noticed that the sensible heat is greatly affected by the outdoor temperature variation. However, the humidity percentage has smaller effect but still considerable as it counts from 18-30 % of the overall heat loss. Also, we have conducted additional studies which involve in altering the ventilation ACH (inlet velocity) and it was found that the latent heat loss is nearly directly proportional to the amount of ambient air entering the building whereas sensible heat losses is almost insensitive.

TABLE 1
Effect of Seasonal Atmospheric Condition on Heat Transfer and Temperature Stratification

Season	Temp. (°C)	RH (%)	Strat.Level (°C)	Sensible heat loss (W)	Latent heat loss (W)
Winter	5	85	0.65	625.3	313
Spring	15	60	0.36	326.2	73
Summer	20	76	0.2	177.5	75
Autumn	10	87	0.5	475.4	232

Given that the rate of evaporation is greatly dependent on temperature and relative humidity of the surrounding[9, 10] a situations as seen in summer and spring conditions, where the building ability to reject heat is significantly reduced, will result in decrease of evaporation rate. Consequently the cooling effect of these ponds would be declined. This observation should be carefully handled as it may increase the cooling water temperature which eventually may lead to overheating raising alarms for emergency.

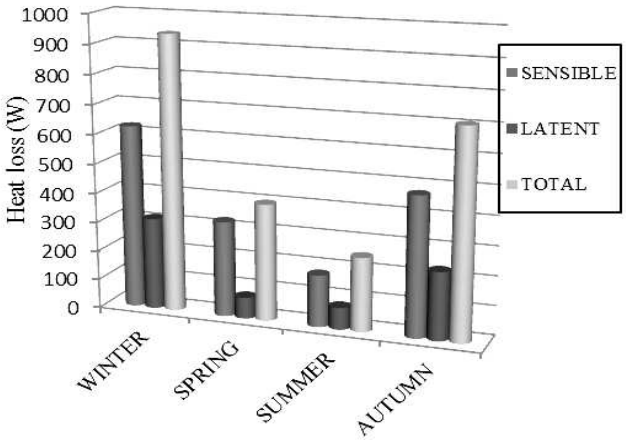

Fig. 12. Sensible and latent heat loss variation under different ambient conditions.

Temperature stratification in the vertical direction along the span of the pool is shown in Fig. 13 where the gradient is monitored on Z-mid plane. It can be clearly seen that the bulk temperature experiences a very small drop except locations X=0.1 and X=0.9 which are influenced by proximity of ventilation inlet and outlet plumes respectively. The volume average temperature is used as a measuring criterion to evaluate stratification level from the water surface to the ceiling. We have observed a minor thermal stratification as listed in Table 1.

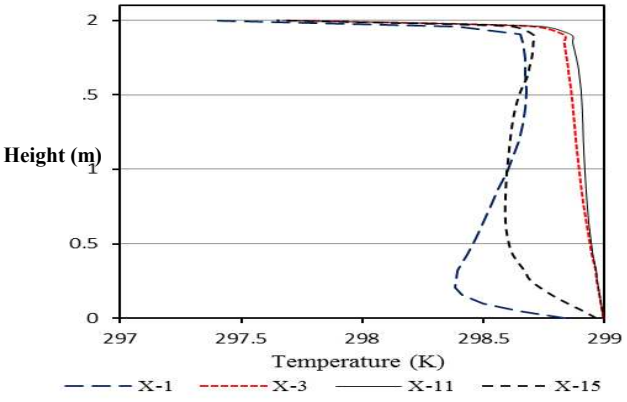

Fig. 13. Vertical temperature gradient on Z-mid plane.

Additional study was performed by changing locations and ACH of the ventilation inlet and outlet. As predicted, very high deviations in temperature distributions were recorded and can be illustrated in Fig.14, for example, increasing inlet velocity by factor of 6. These outcomes agreed reasonably well with those stated by Said et al.[11].

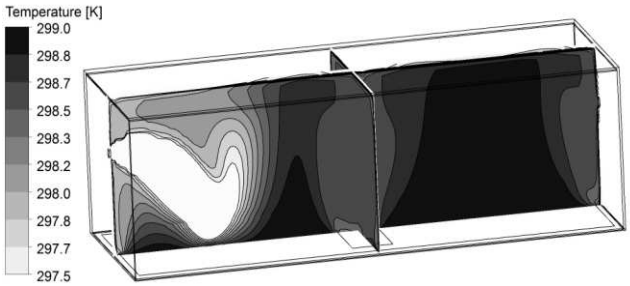

Fig. 14. Temperature gradient on Z-mid and X-mid planes for inlet of 5 m/s.

IV. THERMODYNAMIC APPROACH FOR WORST CASE SCENARIO

Rather than using CFD to consider the worst-case fault situation due to constraints of time, computing power and uncertainty of actual data, overall energy balance approach was used for this study.

The calculations presented in this section represent a scenario when none of the pumps is working. The heat energy released from the spent fuels will continue to be released which will heat up the water. In this very unlikely event the water will start to evaporate. The whole process can be assumed to take place in two stages.

Stage 1

The heat released will increase the temperature of the pool until it reaches the boiling temperature of 100 ^{o}C under normal atmospheric pressure of 101.3 kPa. This is sensible heating and the time required, t_1, to reach this state can be calculated from Eq. (3).

$$t_1 = \rho\, V\, c_p\, (100\text{-}T_{in})/Q \qquad (3)$$

where ρ = density of water; V = volume of water, c_p = specific of water and T_{in} = initial temperature of the pool; Q = Total amount of heat released in watts.

Stage 2

Once the pool of water has reached the saturation temperature of 100 ^{o}C, any further addition of heat from the spent fuel will cause water loss through evaporation which will absorb the latent heat.

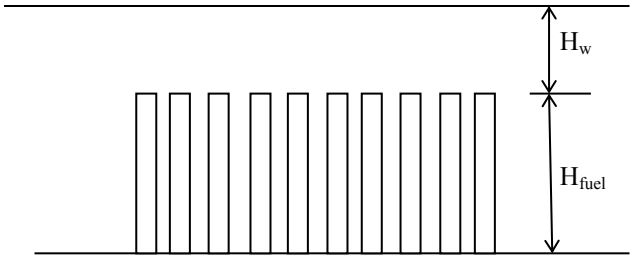

Fig. 14. Schematic of fuel stacking under water for evaporation time calculation.

With reference to the above sketch Fig. 14, H_w represents the water depth on top of the fuel. It can be assumed that as soon as the fuels are exposed due to loss of H_w amount of water, the situation can be termed as critical[1]. The time needed, t_2, for this amount of water to evaporate can be calculated from Eq. (4).

$$t_2 = \rho A H_w (h_g - h_f)/Q, \quad (4)$$

where, A = cross sectional area of the pool, m^2
h_g = enthalpy of steam at saturation temperature
h_f = enthalpy of saturated water
H_{fuel} = 3 m

For a typical pond condition, the following data were generated for different water levels as shown in Table 2 below.

TABLE 2
Drying Time for Different Heights of Water

$H_1=H_{fuel}+H_w$ (metre)	t_1 (days)	t_2 (days)	Total time, $t=t_1+t_2$ (days)
7	4.2	16.6	20.8
6	3.4	12.3	15.7
5	2.7	8.2	10.9

Compared with the details of the CFD, these results may often be misleading for the general public and hence should be treated with utmost caution.

V. CONCLUSIONS

1. CFD in principle can do the full simulation of SNF ponds but has not been tried extensively. One of the reasons is the size of the pond which proves extremely demanding on computing resources. Our methodology has clearly established that the numerical approach can provide very useful insight into the operation of cooling pond.
2. Uncertainty of boundary conditions is an important matter that needs to be properly understood. This is particularly true for evaporation and on how to approximate the atmospheric conditions.
3. The removal of decay heat is achieved in three ways: (a) heat loss by evaporation, (b) heat loss by conduction through the walls and (c) convective heat transfer due to the primary stream. To enable all these boundary conditions implicitly will require even bigger computational domain by accommodating solids and air as part of the domain. The other alternative would be to explicitly specify the individual components, which unfortunately is not accurately known a priori.
4. Results obtained from bulk thermodynamic considerations can be too simplistic and must be treated with caution to avoid uncertainty and misleading negative publicity.
5. One approach to try could be to see the application of porous media approach[12] for closely packed elements. Work is currently underway to categorise various arrangements and to ascertain the accuracy of modelling considering porous media.
6. There is an urgent need to gather experimental data for real life pond conditions. These include temperature data at critical locations along with full details of operational parameters and environmental information. It is possible that such data will allow CFD to be used with confidence and hence will help more efficient and financially competitive business to be operated.

ACKNOWLEDGEMENTS

The authors fully acknowledge the work of Paul Robinson in section 2.

REFERENCES

1. IAEA Nuclear Energy Series. *Costing of spent nuclear fuel storage:* Available from. http://www.iaea.org/sites/default/files/Pub1398_web.pdf (accessed Nov 20, 2014).

2. K. Wang, Y. Guo and He-yi Zeng, *"Spent fuel pool transient analysis under accident case and the flow establishment process of passive cooling system,"* China located International Conference on Information Systems for Crisis Response and Management, Nov. 27-29, 2011.

3. Kim, D., Yook, Se-Jin., Lee, Kwan-Soo. *Investigation of radiative and convective heat transfer in storage vaults for improving space efficiency*. Int. J. Heat and Mass Transfer, 80, 301-308, 2015

4. Yanagi, C., Murase, M., Yoshida Y., Iwaki, T. and Nagae, T. *Evaluation of heat loss and water temperature in a spent fuel pit*, JSME J. Power and Energy Systems, 6(2), 51-62, 2012.

5. Yanagi, C., Murase, M., Yoshida Y., Ultanohara Y., Iwaki, T. and Nagae, T. *Numerical simulation of water temperature in a spent fuel pit during the shutdown of its cooling systems*, JSME J. Power and Energy Systems, 6(3), 423-434, 2012.

6. Robinson, P., R. Hasan, and J. Tudor. *Numerical Simulation of Flow and Heat Transfer in Spent Fuel Cooling Ponds*. in Lecture Notes in Engineering and Computer Science: *Proceedings of the World Congress on Engineering*. 2013, pp. 1861-1864.

7. ANSYS FLUENT 14.0 (2014).

8. Ramadan, A., R. Hasan, and J. Tudor. *Simulation of Flow and Heat Transfer of Humid Air in Spent Fuel Cooling Ponds, Proceedings of the World Congress on Engineering*. 2014, pp. 1508-1512.

9. Vinnichenko, N.A., et al., *Direct computation of evaporation rate at the surface of swimming pool.* Recent Researches in Mechanics, 2O11, 2011: p. 120-124.

10. M. D. Hancock, *"Indoor swimming pools and leisure centres – A model to improve operational effectiveness and reduce environmental impact," CIBSE Technical Symposium, Sept. 6-7, 2011, De Montfort University, Leicester, UK.*

11. Said, M., R. MacDonald, and G. Durrant, *Measurement of thermal stratification in large single-cell buildings.* Energy and buildings, 1996. **24**(2): p. 105-115.

12. Hung, T.-C., et al., *The development of a three-dimensional transient CFD model for predicting cooling ability of spent fuel pools.* Applied Thermal Engineering, 2013. **50**(1): p. 496-504.